Comprehensive Optimization-based Techno-economic Assessment of Hybrid Renewable Electricity-hydrogen Virtual Power Plants

James Naughton, *Member*, *IEEE*, Shariq Riaz, *Senior Member*, *IEEE*, Michael Cantoni, *Member*, *IEEE*, Xiao-Ping Zhang, *Fellow*, *IEEE*, and Pierluigi Mancarella, *Fellow*, *IEEE*

***Abstract*—Hydrogen is being considered as an important option to contribute to energy system decarbonization. However, currently its production from renewables is expensive compared with the methods that utilize fossil fuels. This paper proposes a comprehensive optimization-based techno-economic assessment of a hybrid renewable electricity-hydrogen virtual power plant (VPP) that boosts its business case by co-optimizing across multiple markets and contractual services to maximize its profits and eventually deliver hydrogen at a lower net cost. Additionally, multiple possible investment options are considered. Case studies of VPP placement in a renewable-rich, congested area of the Australian network and based on real market data and relevant sensitivities show that multi-market participation can significantly boost the business case for cleaner hydrogen. This highlights the importance of value stacking for driving down the cost of cleaner hydrogen. Due to the participation in multiple markets, all VPP configurations considered are found to be economically viable for a hydrogen price of 3 AUD $/kg (2.25 USD $/kg), which has been identified as a threshold value for Australia to export hydrogen at a competitive price. Additionally, if the high price volatility that has been seen in gas prices in 2022 (and by extension electricity prices) continues, the flexibility of hybrid VPPs will further improve their business cases.**

***Index Terms*—Virtual power plant, techno-economic assessment, electrolyser, flexibility, hydrogen, multi-energy system, optimal power flow.**

NOMENCLATURE

A. Sets

Ψ^B	Set of lines (branches) of network
Ψ_i^B	Set of lines (branches) connected to node i
Ψ^K	Set of resources in the network
Ψ_i^K	Set of resources at node i
Ψ^H	Set of hydrogen-based resources in the network
Ψ_i^H	Set of hydrogen-based resources at node i
Ψ^E	Set of energy storage resources in the network
Ψ^N	Set of nodes in the network

B. Parameters

α_k, β_k	Allowable curtailments in each time period and across the whole horizon for resource k
γ_k	Operating cost of fixed resource k
Δt	Optimization time step length
$\epsilon_{k,t}$	Available generation (if positive) or demand power (if negative) of resource k
$\zeta_{k,0}$	Initial resource commitment status
η_k^g, η_k^l	Generation and consumption efficiencies of resource k
$\bar{\theta}_i$, $\underline{\theta}_i$	The maximum and minimum nodal voltage angles at node i
λ_k^{curt}	Price of curtailing active power at time t
$\lambda_t^{\text{H}_2}$	Price of hydrogen at time t
λ_k^{on}, λ_k^{off}	Start-up and shut-down costs of resource k
λ_t^{P}, λ_t^{Q}	Prices of wholesale energy and reactive power at time t
$\boldsymbol{\lambda}_t^{\text{Raise}}$, $\boldsymbol{\lambda}_t^{\text{Low}}$	Vectors of raise and lower frequency control ancillary services (FCASs) market prices at time t
λ_t^{renew}	Cost of purchasing previously curtailed renewable energy at time t
v_k	Energy storage losses of resource k
$\bar{\rho}_k$, $\underline{\rho}_k$	The maximum and minimum ramp up capabilities of resource k

Manuscript received: June 8, 2022; revised: August 30, 2022; accepted: October 17, 2022. Date of CrossCheck: October 17, 2022. Date of online publication: October 26, 2022.

The authors would like to acknowledge the partial support of the Victorian Government through the veski initiative and the UK EPSRC through the MYSTORE project (No. EP/N001974/1).

J. Naughton (corresponding author), S. Riaz, M. Cantoni, and P. Mancarella are with the University of Melbourne (UoM), Australia, and J. Naughton is also with the University of Birmingham (UoB), UK, and P. Mancarella is also with the University of Manchester, UK (e-mail: james. naughton@unimelb. edu. au; shariq.riaz@unimelb.edu.au; cantoni@unimelb.edu.au; pierluigi.mancarella@unimelb.edu.au).

X. P. Zhang is with the University of Birmingham (UoB), UK (e-mail: X.P. Zhang@bham.ac.uk).

DOI: 10.35833/MPCE.2022.000324

$\boldsymbol{\sigma}^{\text{Raise}}$, $\boldsymbol{\sigma}^{\text{Low}}$ Vectors of raise and lower FCAS service call times

$\boldsymbol{\tau}^{\text{Raise}}$, $\boldsymbol{\tau}^{\text{Low}}$ Vectors of raise and lower FCAS service durations

$\bar{\varphi}_k$, $\underline{\varphi}_k$ The maximum and minimum active/reactive dispatch power ratios of resource k

Φ_k^{ϵ} Polarity of ϵ_k (−1 if negative and 1 if positive)

Φ_k^{FFR} Generation to be covered by fast frequency response (FFR) of resource k

χ_k^{g}, χ_k^{l} Generation and consumption costs of resource k

$\bar{\omega}_{k,t}$ Active power curtailment when virtual power plant (VPP) is not present of resource k

B_{ij}, G_{ij} Susceptance and conductance of branch ij

E_k Resource k storage capacity

$\bar{H}_i$ Hydrogen storage capacity at node i

H_i^{target} Normalized stored hydrogen target for end of optimization at node i

$\bar{P}_k^{\text{g}}$, $\underline{P}_k^{\text{g}}$ The maximum and minimum active power generations of resource k

$\bar{P}_k^{\text{l}}$, $\underline{P}_k^{\text{l}}$ The maximum and minimum active power consumptions of resource k

$\bar{Q}_k$, $\underline{Q}_k$ The maximum and minimum reactive power of resource k

$\bar{S}_{ij}$ Power flow limit of branch ij

T Number of time steps in optimization

U_k, D_k The minimum "up time" and "down time" of resource k

$\bar{V}_i$, $\underline{V}_i$ The maximum and minimum nodal voltage magnitudes at node i

X_k^{target} Normalized stored energy target of resource k for end of optimization

C. Variables

$\zeta_k(t)$ Commitment status (0 is off and 1 is on) of resource k at time t

$\theta_i(t)$ Nodal voltage angle at node i at time t

$\omega_k(t)$ Active power curtailment of resource k at time t

$c^{\text{tot}}(t)$ Total cost of network operation at time t

$c^{\text{op}}(t)$ Cost of operating resources scheduled at time t

$h_i(t)$ Normalized level of stored hydrogen at node i at time t

$h_i^{\text{d}}(t)$ Amount of hydrogen exported at node i at time t

$p_k(t)$ Active power injection of resource k at time t

$p_{ij}(t)$ Active power flow of branch ij at time t

$p^{\text{ext}}(t)$ Active power imported from power grid at time t

$p_k^{\text{FFR}}(t)$ FFR bid of resource k at time t

$p_k^{\text{g}}(t)$, $p_k^{l}(t)$ Active power generation and consumption of resource k at time t

$\boldsymbol{p}_k^{\text{Low}}(t)$ Vector of all lower FCAS bids of resource k at time t

$\boldsymbol{p}_k^{\text{Raise}}(t)$ Vector of all raise FCAS bids of resource k at time t

$q_k(t)$ Reactive power injection of resource k at time t

$q_{ij}(t)$ Reactive power flow of branch ij at time t

$q^{\text{ext}}(t)$ Reactive power imported from power grid at time t

$V_i(t)$ Nodal voltage magnitude at node i at time t

$x_k(t)$ Normalized level of stored energy of resource k at time t

I. Introduction

OVER the past decades, the focus on reducing the carbon footprint of electrical networks has been addressed by integrating renewable energy sources (RESs) and distributed energy resources (DERs) into the electrical networks. The rapid increase in RESs in turn has led to an increase in curtailed renewable energy. This has led to the emergence of hydrogen generated using renewable energy as a possible energy vector to help phase out fossil fuels. This hydrogen is created by using energy from RES to power an electrolyser. This process releases virtually zero emissions, and the hydrogen can then be used as a fuel source for vehicles [1], injected into a gas network [2], or converted into ammonia or methane for uses in other industries. However, in general, hydrogen generated from RES is much more expensive to create than its carbon-intensive counterparts [3]. It is worth noting that the high and volatile wholesale gas prices that are being experienced worldwide in 2022 are likely to make hydrogen generated from RES more competitive, as hydrogen generated from natural gas will become more expensive. Australia has been investing in hydrogen and has identified that a target hydrogen production price of 2-3 AUD$/kg (excluding storage and transport) is needed for Australia to export hydrogen at a competitive price [4]. This is well below the current levelized cost of hydrogen of 5-7 AUD$/kg calculated in [4]. However, there are operational considerations that can reduce the net production cost of hydrogen.

The rise in RES has also caused a decrease in scheduled thermal generation, which traditionally would supply network services. Therefore, there is an opportunity for new players in the network to fill this gap and provide technical services and collect the associated revenues. Reference [5] concludes that initial investment costs are too large for power-to-gas flexibility to be profitable, although there is limited consideration of the markets and services an electrolyser could participate in. If properly controlled (and potentially aggregated into a virtual power plant (VPP)), an electrolyser could utilize its operational flexibility to provide network services [6], as well as participate in markets and contracts to generate additional revenue [7]. Electrolysers can be used as flexible loads to provide reserve services [8], demand response [9], and network services [10]. This flexibility becomes more valuable with increased price volatility, as seen in 2022 wholesale gas prices, and their knock-on effect on wholesale electricity prices. It has been shown that with the proper operational consideration, a VPP (which could contain an electrolyser) can be used to provide voltage regulation in a distribution system [11], [12], and [13] proposes a VPP that aggregates and controls local PV generation to en-

sure that local thermal and voltage constraints are not violated. One advantage of aggregating an electrolyser into a VPP is that VPPs can better participate in electricity markets, as in [14] where a VPP is proposed to participate in the wholesale energy market by providing energy arbitrage. VPP participation in energy markets can provide a wider system benefit, reducing the overall dispatch cost of a network [15].

Reference [16] highlights the benefits of coupling electrolysers with gas-to-power resources, including the ability to convert hydrogen back to electricity as an additional revenue generating option – although in the case study it is rarely used due to the high price of natural gas. The coupling of electrolysers and fuel cells (FCs) for grid-scale energy storage is examined in [17], which determines it is a viable energy storage option, although the work identifies issues with its low round-trip efficiency compared with battery energy storage. However, that work does not consider its application beyond energy arbitrage. It has been established in previous works that aggregated resources can participate in multiple markets simultaneously [18]. In [19], it is concluded that hydrogen resources as part of a VPP can provide network services and participate in multiple markets. Multi-market participation is of high importance, as doing so can lead to increased revenue [20], [21], which can be critical for resource profitability, especially in increasingly volatile markets. Therefore, the consideration of multi-market participation is key to identifying an accurate estimate of the economic potential of hydrogen resources.

Whilst it has been shown that electrolysers and other hydrogen-based resources can provide network services and participate in markets, previous works on business cases and economic feasibility of integrating hydrogen resources into the electrical networks overlook this. The economic benefits of integrating electrolysers into the electrical network have been studied, often operating in conjunction with RES such as wind farms [22], [23]. However, these works typically overlook the operational aspects of the electrolyser. In fact, many works rely on simple heuristics for the operation of the hydrogen-based resources [24]. This does not provide a true representation of the operation of these hydrogen-based resources. It has been shown in [25] that controlling electrolysers considering current and future RES generation and market conditions yields a better result than steady-state operation. This additional benefit from active control of hydrogen-based resources will increase if the highly volatile prices seen in 2022 for wholesale gas become a more regular occurrence. This then leads to an overall reduction in the net cost of generating hydrogen from RES. Additionally, the modelling of the electrical network is often overlooked [16]. It is shown in [26] that network constraints can have a sizeable impact on an electrolyser's hydrogen generation capability. It is also highlighted that electrolysers can be used as a power flow flexibility option to provide network services. Therefore, it is important to consider network constraints to obtain an accurate estimate of potential revenue. In [27], an electrolyser and wind farm are operated together, and a basic consideration of the electrical network through a transformer thermal rating is included. Even when this limited consideration of network conditions is included, it results in reduced costs and reduced RES curtailment.

It is clear therefore, that to create a high accuracy business case assessment for investing in electrolysers and other hydrogen-based resources, it is important to consider all possible revenue streams these resources could tap into in the electrical network, as well as possible limitations and revenue streams related to the electrical network. It has been shown in previous works that hydrogen resources can provide network services and participate in markets, but the impact of this on the business cases for hydrogen resources and net cost of producing hydrogen is currently lacking in the literature. The references are not aware of any work that provides a business case utilizing a comprehensive techno-economic assessment of hydrogen costs from an electrolyser coordinated in a VPP, that considers the full range of possible markets and services, as well as modeling the electrical network and utilizing current real-world prices. This could help inform the understanding of the true economic potential of hydrogen in the electrical network, which is key to accelerating the advent of the hydrogen economy.

This work considers a number of investment options for hydrogen-based resources with various market/service portfolios and conducts a comprehensive techno-economic assessment of the economic viability of fixed price hydrogen contracts within the context of the Australian energy network. To do this, a deterministic scheduling optimization considering multiple energy vectors is utilized. It is noted that, as there is no spot market for hydrogen in Australia, such as there is for natural gas, the electrolyser operator would need to enter into a sale and purchase agreement (SPA) with a third party who is buying the hydrogen. In this way, the fixed price hydrogen contracts considered in this work are the most likely method of buying and selling large quantities of hydrogen for the foreseeable future.

The optimization used in this work schedules and dispatches a multi-energy VPP participating in markets/contracts for:

1) An intra-day wholesale energy spot market.

2) A fixed-price hydrogen contract/SPA.

3) Six intra-day frequency control ancillary service (FCAS) markets to respond to contingency events to raise or lower network frequency.

4) A voltage control ancillary service (VCAS) in the form of upstream reactive power support.

5) A system restart ancillary service (SRAS) contract (if a resource is invested in which can provide the service).

6) A fast frequency response (FFR) contract with new renewable generators in the network to provide FFR on their behalf.

7) Contractual arrangements with local renewables to buy renewable energy curtailed due to congestion.

The main contributions of this work are:

1) Investigation of the economic viability of possible combinations of an electrolyser, hydrogen storage, fuel cells, and hydrogen-powered open cycle gas turbine (OCGT), for a fixed-price hydrogen contract/SPA compared with battery energy storage (as a current popular choice for utility energy storage which can also provide network services).

2) Presentation of comprehensive business cases assessing investment options for hydrogen-based resources considering the full range of markets and services, and the impacts of electrical network constraints.

3) A robust business case for the hydrogen-electricity VPP informed by sensitivity analysis of multiple market prices and magnitude of contractual services.

The rest of the paper is structured as follows. Section II presents the methodology used for the techno-economic assessments in this work. Section III outlines the case study to which the methodology is applied, based on the introduction of an electricity-hydrogen VPP into a renewable-rich area of the network. Section IV provides the results from the case study, and Section V summarizes the findings of this work.

II. Methodology

The VPP modelling conducts a unit commitment utilizing multi-service, multi-energy optimal power flow studies for maximizing the profit of a VPP participating in multiple markets [19]. It is noted that, while the modelling considers multiple energy vectors, it only models the flow of electrical energy. Other energy vectors (in this case study, hydrogen) have their imports and exports balanced at each node. The VPP is a subset of the devices in the network. The operation of other devices in the network (load and generation) is also included in the optimization to model how these devices would interact with the VPP and respond to market prices and network congestion.

The centralized approach to the optimization proposed in this work with the VPP acting as a price-taker internalizes the real-world two-stage interaction between the VPP (and other commercial entities) and the market operator by having the VPP operator anticipate the network constraints and respond accordingly. This allows the commercial planning problem to be solved without modelling the full bidding process, but still factoring network constraints and market prices into the VPP operation.

The electrical power flows are modelled using a decoupled linear power flow model [28]. The market and products that are modelled in this work include: a wholesale energy market; VCAS in the form of upstream reactive power support; hydrogen in the form of a fixed-price contract; raise and lower FCAS services with 6 s, 60 s, and 5 min response time; FFR; and contractual arrangements between the VPP and RES to buy their curtailed power.

The optimization proposed is deterministic. As part of this planning problem, it is assumed that the VPP operating close-to-real-time will have good information on which to base its operation. Previous works have shown how a VPP operating close-to-real-time can effectively respond to uncertainty through receding horizon control, minimizing the loss in VPP revenue due to uncertainty [29]. Additionally, for close-to-real-time operation, the VPP may have access to forecasts of renewable generation as part of the contracts it holds with renewable generators, reducing the VPP operator's uncertainty regarding RES generation.

VPP operation is optimized across the time horizon $[1{:}T]$, in steps of length Δt. Throughout, subscript t denotes a time-varying parameter, whilst $*(t)$ denotes a variable's value at time t. The subscript k denotes the corresponding instance of a parameter or decision variable for specific resource k. The subscript i denotes the corresponding instance of a parameter or decision variable for specific node i.

A unit commitment model with linearized power flow constraints and fixed generation cost is used in this work, as is typical in such studies [30]. The unit commitment model proposed in this work is also augmented with multi-energy and multi-market/service constraints. This results in a mixed-integer linear program (MILP) that can be readily solved using off-the-shelf software. The optimization consists of equality and inequality constraints that encode the objective function (1) and network and resource characteristics (see (2)-(47) below).

The objective function (1) is a sum of the cost (2) over each time step, where $T=48$ hours and $\Delta t=0.5$ hour is the time step length of the optimization (resulting in a 24-hour horizon with 30-minute resolution).

$$\min \sum_{t=1}^{T} c^{\mathrm{tot}}(t)\,\Delta t \tag{1}$$

$$c^{\mathrm{tot}}(t) = \overbrace{\lambda_t^{\mathrm{P}} p^{\mathrm{ext}}(t)}^{\mathrm{I}} + \overbrace{\lambda_t^{\mathrm{Q}} q^{\mathrm{ext}}(t)}^{\mathrm{II}} - \overbrace{\lambda_t^{\mathrm{H_2}} \sum_{i \in \Psi^N} h_i^{\mathrm{d}}(t)}^{\mathrm{III}} + \overbrace{c^{\mathrm{op}}(t)}^{\mathrm{IV}} + \sum_{k \in \Psi^K} \left(\overbrace{\lambda_k^{\mathrm{curt}} \omega_k(t)}^{\mathrm{V}} - \overbrace{\boldsymbol{\lambda}_t^{\mathrm{Raise}} \boldsymbol{p}_k^{\mathrm{Raise}}(t)}^{\mathrm{VI}} - \overbrace{\boldsymbol{\lambda}_t^{\mathrm{Low}} \boldsymbol{p}_k^{\mathrm{Low}}(t)}^{\mathrm{VII}} + \overbrace{\lambda_k^{\mathrm{renew}} \left(\max\left\{ (\bar{\omega}_{k,t} - \omega_k(t), 0 \right\} \right)}^{\mathrm{VIII}} \right) \tag{2}$$

The VPP cost $c^{\mathrm{tot}}(t)$ in (2) comprises eight terms: terms I and II represent buying active and reactive power from the power grid $p^{\mathrm{ext}}(t)$ and $q^{\mathrm{ext}}(t)$, respectively; term III represents the revenue (negative cost) from selling hydrogen, where $h_i^{\mathrm{d}}(t)$ is the hydrogen sold at each node; term IV represents the cost of operating the scheduled resources $c^{\mathrm{op}}(t)$ as encoded by (3); term V represents the cost of curtailment $\omega_k(t)$; terms VI and VII represent the revenue from raise FCAS service bids $\boldsymbol{p}_k^{\mathrm{Raise}}(t)$ and lower FCAS service bids $\boldsymbol{p}_k^{\mathrm{Low}}(t)$, respectively; and term VIII is the cost of purchasing curtailed renewable generation $\bar{\omega}_{k,t}$, which allows the optimization to consider a link between the VPP and RES in congested locations. A well placed VPP can buy energy from an RES that would otherwise be curtailed due to upstream line congestion.

The resource operating cost is encoded by the constraint:

$$c^{\mathrm{op}}(t) \geq \sum_{k \in \Psi^K} \left(\chi_k^{\mathrm{g}} p_k^{\mathrm{g}}(t) + \chi_k^{\mathrm{l}} p_k^{\mathrm{l}}(t) + \gamma_k \zeta_k(t) + \frac{\lambda_k^{\mathrm{on}}}{\Delta t} \max\left(0, \zeta_k(t) - \zeta_k(t-1)\right) + \frac{\lambda_k^{\mathrm{off}}}{\Delta t} \max\left(0, \zeta_k(t-1) - \zeta_k(t)\right) \right) \tag{3}$$

where $\zeta_k(0) = \zeta_{k,0}$ is the committed status of resources in the time step before the optimization. There is a cost associated with the power generated by each resource $p_k^{\mathrm{g}}(t)$, the power

demanded by each resource $p_k^{\mathrm{l}}(t)$, as well as a turn-on and turn-off cost.

1) Electrical Network Constraints

The optimization problem includes the following linearized power flow constraints for $t=[1{:}T]$:

$$-\sqrt{2}\,\bar{S}_{ij} \le p_{ij}(t)+q_{ij}(t) \le \sqrt{2}\,\bar{S}_{ij} \quad \forall (i,j) \in \Psi^B \tag{4}$$

$$-\sqrt{2}\,\bar{S}_{ij} \le p_{ij}(t)-q_{ij}(t) \le \sqrt{2}\,\bar{S}_{ij} \quad \forall (i,j) \in \Psi^B \tag{5}$$

$$-\bar{S}_{ij} \le p_{ij}(t) \le \bar{S}_{ij} \quad \forall (i,j) \in \Psi^B \tag{6}$$

$$-\bar{S}_{ij} \le q_{ij}(t) \le \bar{S}_{ij} \quad \forall (i,j) \in \Psi^B \tag{7}$$

$$p_{ij}(t)+p_{ji}(t)=0 \quad \forall (i,j) \in \Psi^B \tag{8}$$

$$q_{ij}(t)+q_{ji}(t)=0 \quad \forall (i,j) \in \Psi^B \tag{9}$$

$$\underline{V}_i \le V_i(t) \le \bar{V}_i \quad i \in \Psi^N \tag{10}$$

$$\underline{\theta}_i \le \theta_i(t) \le \bar{\theta}_i \quad i \in \Psi^N \tag{11}$$

$$p_{ij}(t)=G_{ij}\big(V_i(t)-V_j(t)\big)-B_{ij}\big(\theta_i(t)-\theta_j(t)\big) \quad \forall (i,j) \in \Psi^B \tag{12}$$

$$q_{ij}(t)=-B_{ij}\big(V_i(t)-V_j(t)\big)-G_{ij}\big(\theta_i(t)-\theta_j(t)\big) \quad \forall (i,j) \in \Psi^B \tag{13}$$

$$\sum_{(i,j)\in\Psi_i^B} p_{ij}(t) = \sum_{k\in\Psi_i^K} p_k(t) \quad i \in \Psi^N \tag{14}$$

$$\sum_{(i,j)\in\Psi_i^B} q_{ij}(t) = \sum_{k\in\Psi_i^K} q_k(t) \quad i \in \Psi^N \tag{15}$$

The active and reactive branch power flows, $p_{ij}(t)$ and $q_{ij}(t)$, respectively, are constrained in (4)-(7) by a linear approximation of the non-linear power-flow relationship. This linearization includes neglecting network losses. This is shown in (8) and (9) where the power flow through a line in each direction has the same magnitude, but opposite polarity. The nodal voltage magnitude $V_i(t)$ and angle limit $\theta_i(t)$ are set in (10) and (11), respectively. In (12) and (13), the active and reactive power flows in each line are defined as a function of nodal voltages. Equations (14) and (15) ensure that the active and reactive power injected by resources into a node, i.e., $p_k(t)$ and $q_k(t)$, matches the power flowing out of the node. The point of common coupling is the slack node in the system.

2) Resource Constraints

The resource modelling is encoded by the following additional constraints for $t=[1{:}T]$:

$$\sum_{m=t}^{t+U_k-1} \zeta_k(m) \ge U_k\big(\zeta_k(t)-\zeta_k(t-1)\big) \quad \forall k \in \Psi^K \tag{16}$$

$$\sum_{m=t}^{t+D_k-1} \big(1-\zeta_k(m)\big) \ge D_k\big(\zeta_k(t-1)-\zeta_k(t)\big) \quad \forall k \in \Psi^K \tag{17}$$

$$\zeta_k(t)\,\underline{P}_k^{\mathrm{g}} \le p_k^{\mathrm{g}}(t) \le \zeta_k(t)\,\bar{P}_k^{\mathrm{g}} \quad \forall k \in \Psi^K \tag{18}$$

$$\zeta_k(t)\,\underline{P}_k^{\mathrm{l}} \le p_k^{\mathrm{l}}(t) \le \zeta_k(t)\,\bar{P}_k^{\mathrm{l}} \quad \forall k \in \Psi^K \tag{19}$$

$$p_k(t)=p_k^{\mathrm{g}}(t)-p_k^{\mathrm{l}}(t) \quad \forall k \in \Psi^K \tag{20}$$

$$-\underline{P}_k^{\mathrm{g}}\big(1-\zeta_k(t)\big)+\underline{\rho}_k\Delta t \le p_k^{\mathrm{g}}(t)-p_k^{\mathrm{g}}(t-1) \quad \forall k \in \Psi^K \tag{21}$$

$$-\underline{P}_k^{\mathrm{l}}\big(1-\zeta_k(t)\big)+\underline{\rho}_k\Delta t \le p_k^{\mathrm{l}}(t)-p_k^{\mathrm{l}}(t-1) \quad \forall k \in \Psi^K \tag{22}$$

$$p_k^{\mathrm{g}}(t)-p_k^{\mathrm{g}}(t-1) \le \bar{\rho}_k\Delta t+\bar{P}_k^{\mathrm{g}}\big[1-\zeta_k(t-1)\big] \quad \forall k \in \Psi^K \tag{23}$$

$$p_k^{\mathrm{l}}(t)-p_k^{\mathrm{l}}(t-1) \le \bar{\rho}_k\Delta t+\bar{P}_k^{\mathrm{l}}\big[1-\zeta_k(t-1)\big] \quad \forall k \in \Psi^K \tag{24}$$

$$\zeta_k(t)\,\underline{Q}_k \le q_k(t) \le \zeta_k(t)\,\bar{Q}_k \quad \forall k \in \Psi^K \tag{25}$$

$$p_k(t)\,\underline{\varphi}_k \le q_k(t) \le p_k(t)\,\bar{\varphi}_k \quad \forall k \in \Psi^K \tag{26}$$

$$0 \le x_k(t) \le 1 \quad \forall k \in \Psi^K \tag{27}$$

$$X_k^{\mathrm{target}} \le x_k(T+1) \quad \forall k \in \Psi^K \tag{28}$$

$$0 \le \Phi_k^{\epsilon}\omega_k(t) \quad \forall k \in \Psi^K \tag{29}$$

$$0 \le \alpha_k\big|\epsilon_{k,t}\big| - \big|\omega_k(t)\big| \quad \forall k \in \Psi^K \tag{30}$$

$$\sum_{t=1}^{T}\big|\omega_k(t)\big| \le \beta_k \sum_{t=1}^{T}\big|\epsilon_{k,t}\big| \quad \forall k \in \Psi^K \tag{31}$$

$$E_k\big(x_k(t+1)-x_k(t)\big) = \left(\eta_k^{\mathrm{l}}p_k^{\mathrm{l}}(t)-\frac{p_k^{\mathrm{g}}(t)}{\eta_k^{\mathrm{g}}}+\epsilon_{k,t}-\omega_k(t)-v_k\right)\Delta t \quad \forall k \in \Psi^K \tag{32}$$

$$\bar{H}_i\big(h_i(t+1)-h_i(t)\big) = \left[\sum_{k\in\Psi_i^H}\left(\eta_k^{\mathrm{l}}p_k^{\mathrm{l}}(t)-\frac{p_k^{\mathrm{g}}(t)}{\eta_k^{\mathrm{g}}}-v_k\right)-h_i^{\mathrm{d}}(t)\right]\Delta t \quad \forall i \in \Psi^N \tag{33}$$

$$H_i^{\mathrm{target}} \le h_i(T+1) \quad \forall i \in \Psi^N \tag{34}$$

where $x_k(1)=x_{k,1}$, $h_i(1)=h_{i,1}$, $p_k^{\mathrm{g}}(0)=p_{k,0}^{\mathrm{g}}$, and $p_k^{\mathrm{l}}(0)=p_{k,0}^{\mathrm{l}}$ are the initial values for the normalized level of stored electrical energy for each resource $x_k(t)$, the normalized level of stored hydrogen at each node $h_i(t)$, and the active power generated or demanded by each resource, respectively. The minimum "up time" and "down time" of devices are constrained in (16) and (17). Device active power generation and demand limits are constrained in (18) and (19), respectively. Equation (20) defines the net active power injection of each device. Ramping constraints are defined in (21)-(24). The reactive power limits are defined in (25), and a term that limits the power factor of resources is defined in (26). The normalized level of stored energy of each device is constrained in (27), and the stored energy at the end of the day must be greater than a set threshold as stated in (28). Further, (29) defines the polarity of curtailment of each resource depending on if it is a load or generator, and the curtailment that can occur in each time step and across the whole optimization horizon is constrained in (30) and (31), respectively. Device energy conservation is defined by (32).

A hydrogen network is not modelled in this optimization, as there is not one currently in place in Australia. It is noted that in Australia, if there exists a natural gas distribution network nearby, the hydrogen can be injected into this network. If the VPP were to be paid for the amount of hydrogen injected into the natural gas network, from a VPP perspective, the model proposed in this work could also be used. Howev-

er, modelling the flow of hydrogen in the natural gas network is an area of ongoing research [31], but is beyond the scope of this work. Furthermore, the target cost of generating hydrogen in [4] is considered excluding transport. Therefore, the approach of this work is aligned with that of other works. It is assumed that the VPP has a fixed price contract to supply hydrogen to a third party. So, hydrogen generated can either be sent to a buffer storage tank (which can then be turned back into electricity) or supplied to the third party. Therefore, only the balance of hydrogen at each node is considered in (33), and a target for stored hydrogen at each node at the end of the day is encoded by (34).

3) Market Participation and Service Provision

In addition to buying/selling electrical energy and selling hydrogen, the resources can also participate in other markets and provide services to the network. Their ability to do so is dependent on their ramping capability as well as their power and energy headroom/footroom. For example, for a fuel cell to increase its active power output to provide a network service, there must be sufficient hydrogen reserves to perform this operation.

The contribution of each resource to providing network services is constrained as follows. For $t=[1{:}T]$,

$$0\le \boldsymbol{p}_k^{\text{Raise}}(t)\le \bar{\rho}_k \boldsymbol{\sigma}^{\text{Raise}} \quad \forall k\in\Psi^K \tag{35}$$

$$0\le \boldsymbol{p}_k^{\text{Low}}(t)\le -\underline{\rho}_k \boldsymbol{\sigma}^{\text{Low}} \quad \forall k\in\Psi^K \tag{36}$$

$$\zeta_k(t)\bar{P}_k^{\text{g}}\ge p_k(t)+\max\left(\boldsymbol{p}_k^{\text{Raise}}(t)\right)+p_k^{\text{FFR}}(t) \quad \forall k\in\Psi^K \tag{37}$$

$$-\zeta_k(t)\bar{P}_k^{\text{l}}\le p_k(t)-\max\left(\boldsymbol{p}_k^{\text{Low}}(t)\right) \quad \forall k\in\Psi^K \tag{38}$$

$$E_k x_k(t)\ge \frac{1}{\eta_k^{\text{g}}}\left(p_k^{\text{l}}(t)\Delta t+\boldsymbol{p}_k^{\text{Raise}}(t)\boldsymbol{\tau}^{\text{Raise}}\right) \quad k\in\Psi^E \tag{39}$$

$$E_k\left(1-x_k(t)\right)\ge \eta_k^{\text{l}}\left(p_k^{\text{l}}(t)\Delta t+\boldsymbol{p}_k^{\text{Low}}(t)\boldsymbol{\tau}^{\text{Low}}\right) \quad k\in\Psi^E \tag{40}$$

$$E_k x_k(t+1)\ge \frac{1}{\eta_k^{\text{g}}}\left(p_k^{\text{l}}(t)\Delta t+\boldsymbol{p}_k^{\text{Raise}}(t)\boldsymbol{\tau}^{\text{Raise}}\right) \quad k\in\Psi^E \tag{41}$$

$$E_k\left(1-x_k(t+1)\right)\ge \eta_k^{\text{l}}\left(p_k^{\text{l}}(t)\Delta t+\boldsymbol{p}_k^{\text{Low}}(t)\boldsymbol{\tau}^{\text{Low}}\right) \quad k\in\Psi^E \tag{42}$$

$$\bar{H}_i h_i(t)\ge \sum_{k\in\Psi_i^H}\frac{1}{\eta_k^{\text{g}}}\boldsymbol{p}_k^{\text{Raise}}(t)\boldsymbol{\tau}^{\text{Raise}} \quad \forall i\in\Psi^N \tag{43}$$

$$\bar{H}_i h_i(t+1)\ge \sum_{k\in\Psi_i^H}\frac{1}{\eta_k^{\text{g}}}\boldsymbol{p}_k^{\text{Raise}}(t)\boldsymbol{\tau}^{\text{Raise}} \quad \forall i\in\Psi^N \tag{44}$$

$$\bar{H}_i\left(1-h_i(t)\right)\ge \sum_{k\in\Psi_i^H}\eta_k^{\text{l}}\boldsymbol{p}_k^{\text{Low}}(t)\boldsymbol{\tau}^{\text{Low}} \quad \forall i\in\Psi^N \tag{45}$$

$$\bar{H}_i\left(1-h_i(t+1)\right)\ge \sum_{k\in\Psi_i^H}\eta_k^{\text{l}}\boldsymbol{p}_k^{\text{Low}}(t)\boldsymbol{\tau}^{\text{Low}} \quad \forall i\in\Psi^N \tag{46}$$

$$\sum_{k\in\Psi^{\text{FFR}_s}}p_k^{\text{FFR}}(t)-\sum_{k\in\Psi^{\text{FFR}_d}}\Phi_k^{\text{FFR}}p_k(t)\ge 0 \tag{47}$$

where $\max(\boldsymbol{v})$ denotes the maximum element of the vector argument $\boldsymbol{v}$. Each resource's network service response capability is constrained by its ramp rate in (35) and (36), and its maximum and minimum power in (37) and (38), respectively. If the resource has electrical storage, its response is also limited by its available energy storage headroom/footroom in (39)-(42). Note that the energy capacity requirements in (39)-(42) are restricted to the set of resources $\Psi^E\subset\Psi^K$ that accommodate energy storage. Likewise, if it is a hydrogen-based device, it is constrained by the headroom/footroom in the node's hydrogen storage (43)-(46). Further, (47) ensures that the amount of FFR provided by the VPP meets the contracted amount. The sets of resources $\Psi^{\text{FFR}_s}\subset\Psi^K$ and $\Psi^{\text{FFR}_d}\subset\Psi^K$ denote resources that supply/demand FFR services, respectively.

To summarize, the problem is to minimize (1) over the quantities labelled "variables" in the nomenclature section, e.g., $\zeta_k(t)$, $c^{\text{tot}}(t)$ with $T=48$ hours, $\Delta t=0.5$ hour, subject to (2)-(47). This is run for each day in a year to determine annual operational results.

III. Case Study

The case study used in this paper is based on an area of the South Australian (SA) network that is weakly linked to the rest of the power grid. Currently it consists of three distribution substations, two thermal open cycle gas turbines (OCGTs) (50 MW and 23 MW) and two wind farms (~70 MW). For this case study, the network has been supplemented with additional RES in the form of two 30 MW PV solar farms which are under consideration for installation, as shown in Fig. 1. These resources are in the network, but not part of the VPP.

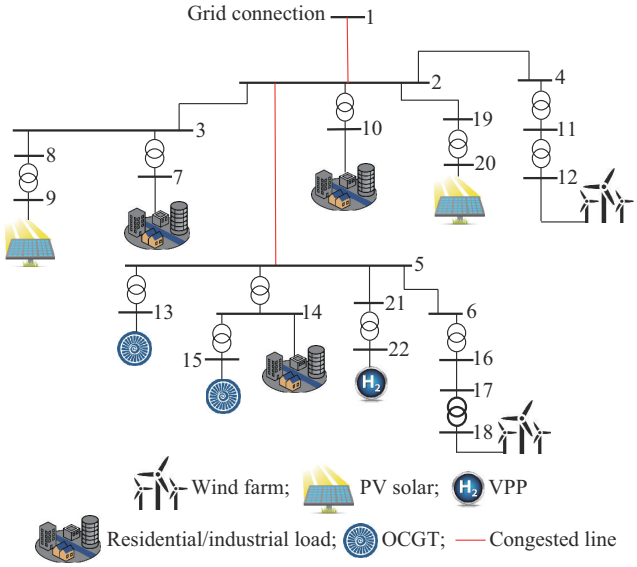

Fig. 1. Diagram of network and position of proposed VPP.

The local area is home to large export facilities for shipping goods to international destinations. This is a prime location for hydrogen generation for international distribution, as this minimizes domestic transportation requirements. For this case study, the modelling approach is utilized by a potential VPP owner, and the inclusion of network constraints in the model allows them to understand the possible impact that the electrical network may have on their operation when the market operator is dispatching resources. This includes identifying where there may be potential for agreements with renewables to purchase their energy that would otherwise be curtailed, or to understand if there may be existing network

constraints that could limit their ability to be dispatched. Information on constraints in the national electricity market dispatch engine, as well as resource bids and dispatch instructions are publicly available from the Australian Energy Market Operator (AEMO). The case study will consider the techno-economic benefits of installing an electricity-hydrogen VPP in the local network, using an electrolyser to generate hydrogen to sell to a third party. To reduce the net cost of generating this hydrogen, the VPP will also participate in additional markets and services. Possible resources to be included in the VPP are a battery energy storage system (BESS), electrolyser, FC, hydrogen OCGT, and hydrogen storage.

The position of these resources in the network, as well as the general network configuration, is shown in Fig. 1. Only the resources located at node 22 are part of the proposed VPP. It is assumed that the other generators are owned and operated by other entities. The lines running between nodes 1-2 and 2-5 have been identified as points of congestion that limit the export of the RES in the network, so that the case study can assess the technical implications of different VPP configurations (installing different combinations of resources in the VPP), and all of the resources and the network in Fig. 1 are included in the optimization detailed in Section II. Each non-VPP resource is assumed to participate only in the wholesale energy market, emulating each resource responding to economic incentives, and so providing a good indication of the state of the network, which may inhibit VPP operation.

A. Cost of Resources in VPP

To be able to fully consider the profitability of the VPP, it is not sufficient to only consider the revenue that the VPP accrues from operating in markets. The investment over the lifetime of the devices including capital expenditure (CAPEX) and operational expenditure (OPEX) should be considered to determine how much revenue the VPP needs to obtain. In this case study, it is assumed that the VPP operator will own all of the resources in the VPP. The devices that may be included in the VPP are shown in Table I. This table contains the capital and operational costs of the devices in the VPP. Note that all costs and revenues in this work are in Australian dollars (1 AUD$ ≈ 0.7 USD$).

TABLE I
EQUIVALENT ANNUAL COSTS (EACS) OF DEVICES IN VPP

Device	Capital investment	Fixed operation & maintenance	Size	CAPEX (M$)	OPEX per year (k$)	Lifetime (year)	EAC (M$)
BESS [32]	813 $/kW+543 $/kWh	10 $/(kW·year)	30 MW/8 MWh	28.734	300	20	3.012
Proton exchange membrane (PEM) electrolyser [33], [34]	1400 $/kW	54 $/(kW·year)	30 MW	42.000	1620	20	5.585
Hydrogen OCGT [34]	1250 $/kW	12.6 $/(kW·year)	10 MW	12.500	126	40	1.064
Hydrogen FC [4]	2109 $/kW	58 $/(kW·year)	5 MW	10.545	290	20	1.285
Hydrogen storage [4]	1032 $/(kg·day)	22 $/(kg·day)	11475 kg/day	11.842	252	40	1.140

The EAC represents the annual cost of owning, operating, and maintaining an asset. It is especially useful for comparing costs of assets with differing lifespans. The EAC is calculated as:

$$EAC = \frac{CAPEX \cdot d}{1 - (1+d)^{-n}} + OPEX \tag{48}$$

where d is the discount rate set to be 7%; and n is the asset lifetime.

For this case study, the hydrogen storage capability is sized to be able to store 11475 kg of hydrogen each day. This size is calculated based on a 30 MW electrolyser operating with a capacity factor of 85% [4], an assumed efficiency of 75%, and the higher heating value of hydrogen as 40 kWh/kg. Seven different VPP configurations are considered in this work. These configurations and EACs are detailed in Table II.

B. Services and Markets

There are 28 case studies considered in this work, utilizing seven VPP configurations and four market/service portfolios. A VPP with Portfolio A would participate in wholesale energy, curtailed RES, and hydrogen markets. Portfolio B includes all markets of Portfolio A as well as contingency FCAS markets. Portfolio C includes all markets of Portfolio B as well as provision of FFR. Portfolio D includes all markets and services of Portfolio C, and additionally includes VCAS and SRAS.

TABLE II
EAC OF EACH OF POSSIBLE VPP CONFIGURATIONS

Case	Resource	EAC (M$)
1	BESS	3.01
2	Electrolyser + hydrogen storage	6.73
3	Electrolyser + hydrogen storage + FC	8.01
4	Electrolyser + hydrogen storage + OCGT	7.79
5	Electrolyser + hydrogen storage + FC+ OCGT	9.08
6	Electrolyser + hydrogen storage + FC +OCGT + BESS	12.09
7	Electrolyser + hydrogen storage + FC + BESS	11.02

Past wind generation profiles and wholesale energy and FCAS prices are provided by AEMO [35]. Past solar irradiance data are provided by the Australian Bureau of Meteorology [36]. Substation load data are provided by South Australia Power Networks [37].

1) Wholesale Energy

The optimization problem in Section II relates to maximiz-

ing revenue from energy exchange at the grid connection point in Fig. 1. The value that the VPP derives from the wholesale energy market can be found by considering the power injection/absorption of the VPP's constituent devices (not taking into account the energy that is coming from the contractual relationship with RES described in this subsection) and utilizing the marginal loss factor associated with the VPP location in the network. The cost of network support payments such as transmission use of system charges have not been included in this analysis. In the National Electricity Rules, it states that when negotiating the amount of network support payment owed by an Embedded Generator, the network services it provides and the avoided customer TUoS charges must be taken into account [38]. It is therefore assumed that network support payment can be disregarded in this work.

2) Curtailed Renewables

Due to the remote location of this area of the network, and the high potential of renewables, there are times when RES generation is curtailed due to line thermal limits being reached. In this work, the VPP can purchase this energy that would otherwise be curtailed from RES for a price of 30 $/MWh.

3) Hydrogen

In these case studies, hydrogen is sold as part of a fixed-price contract. Prices of 2-3 $/kg (excluding storage and transport) have been identified as the target price region for Australia to be able to compete with other exporting countries [4]. In this work, we consider two alternatives for the hydrogen fixed-price contracts, 2 $/kg and 3 $/kg. Whilst for this case study, a fixed-price contract for the sale of hydrogen is considered most appropriate, if in the future hydrogen is traded in sufficiently large quantities, a hydrogen market may be established. Whilst this market is still likely to be dominated by contracts for production of hydrogen, this could lead to hydrogen prices that vary with time. The proposed formulation is flexible enough to model time-varying hydrogen prices, as might be seen in a future hydrogen market.

4) Contingency FCASs

Contingency FCASs are the services to help the network cope with a sudden change in network load or generation (a contingency event), and in Australia, are divided into two sets of services. Contingency raise FCAS services are used to raise the system frequency and are divided depending on the required response time into fast (6 s), slow (60 s) and delayed services (300 s). In addition, there are also fast, slow, and delayed lower FCAS services with the same response time requirements that are used to lower the system frequency after a contingency. There are then six contingency FCAS markets that the VPP can choose to participate in.

5) FFR

FFR in the Australian network is defined as "the delivery of a rapid active power increase or decrease by generation or load in a timeframe of two seconds or less" [39]. AEMO is currently considering placing obligations to provide FFR on new RES [40]. Traditionally, this would mean that the RES would need to install some form of storage (such as a BESS) to be able to provide such a service or contract the provision of FFR out to a third party. This third party could be a curtailable load. If the renewable generator is called to provide FFR, the curtailable load can instead reduce its power output, having the same net results. In this case study, it is considered that the two PV farms are newly connected RESs, and as such are required to provide FFR. Two magnitudes of FFR are considered in this case study. One where the FFR provided must be 50% of the power generated by the PV farms, and the other where the FFR requirement is only 33%. This is used to provide sensitivity analysis to the magnitude of this contractual agreement. The yearly contract value for providing FFR is assumed to be 50% of the EAC of procuring a battery suitable to provide FFR. This equates to 1506000 $/year.

6) VCAS

AEMO maintains voltage levels across the transmission network within relevant limits. This can be done by absorbing or injecting reactive power into transmission network connection points [41]. High system voltages during periods of lower demand (e.g., overnight) are an emerging system issue which can be addressed by dispatching reactive power devices to absorb reactive power. From 2015 to 2019, AEMO had a contract for 800 Mvar absorbing reactive power VCAS with a network service provider (NSP) [42] worth approximately 10 M $ per year. The increase in inverter-based DER provides NSPs an alternate avenue for sourcing reactive power absorption to provide VCAS. VCAS in this case study is assumed to be a market structure, where the VPP injects/absorbs reactive power in response to price signals from an NSP or other entity. Reactive power price signals are used to incentivize the absorption of reactive power during 22:00-05:00 at a fixed price of 1 $/(Mvar·h).

7) SRAS

In the Australian system, the provision of black-start services falls into SRAS. Each subsection of the Australian system is assessed on the magnitude of SRAS that it requires. For the SA system, this is 330 MW [43]. Each year, AEMO publishes the costs of providing SRAS for each subsection [44]. By averaging the amount paid for this 330 MW of SRAS in SA over the past 7 years, the cost of procuring SRAS in SA can be estimated as 10300 $/(MW·year). The hydrogen OCGT considered in this work can provide SRAS. Therefore, when it is part of the proposed VPP, the VPP has the ability to provide 10 MW (the size of the hydrogen OCGT) of SRAS, which is estimated to be valued at 103000 $/year.

C. Feasible Operating Region (FORs) of VPP

A VPP can participate in markets and provide services by utilizing its electrical flexibility – a measure of the capability of a VPP to deviate from a set dispatch point. Flexibility maps, created using the approach proposed in [6], are used to visualize VPP flexibility via FORs. The FOR shows the set of all feasible power dispatch points of the VPP. These are created considering the active, reactive, and apparent power operational constraints of resources in the VPP. The feasibility maps of each of the seven VPP configurations are

shown in Fig. 2, in *Q*-*P* space and H_2-*P* space, where negative values indicate absorption/consumption and positive values indicate generation/injection. The discontinuities in the FORs arise from switching of resources with the minimum operating power requirements.

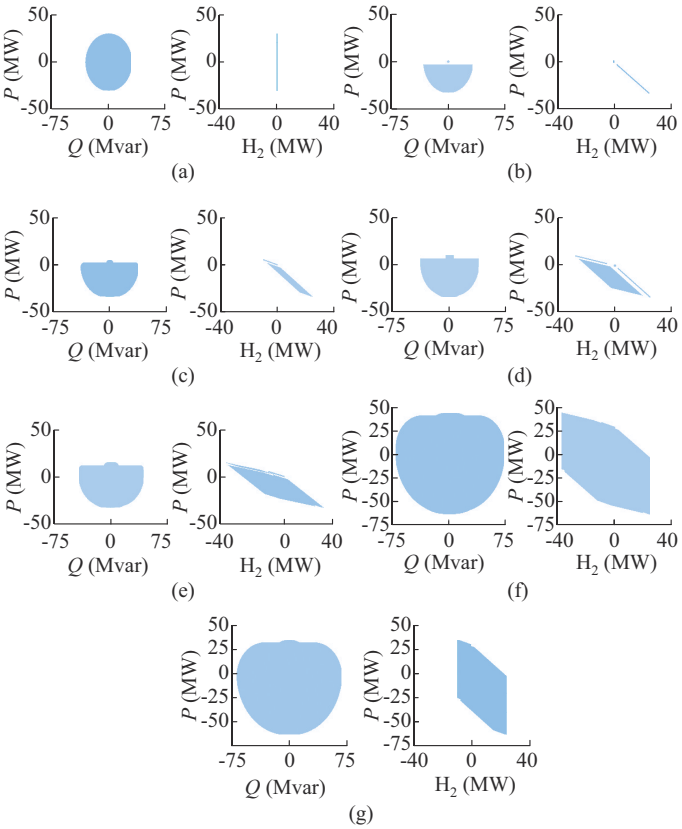

Fig. 2. Feasibility maps of each of seven VPP configurations in *Q*-*P* space and H_2-*P* space. (a) Case 1. (b) Case 2. (c) Case 3. (d) Case 4. (e) Case 5. (f) Case 6. (g) Case 7.

Electrical flexibility can be considered as either upward flexibility (the ability of a VPP to increase its active power injection or consume less active power) or downward flexibility (the ability of a VPP to decrease its active power injection or consume more active power). The amount of upward and downward flexibility that is available to the VPP at a specific time is dependent upon its dispatch point. For example, for the VPP in Case 2 (the electrolyser) to provide 10 MW of upward flexibility (for example to provide FFR), it must be operating with an active power dispatch point no greater than −10 MW, forcing it to absorb power while providing the service. However, if the VPP in Case 5 (electrolyser, fuel cell, and hydrogen OCGT) were providing that same 10 MW of upward flexibility, it would only need to have an active power dispatch less than 5 MW (assuming reactive power dispatch is 0 Mvar and all resources are on). Therefore, in Case 5, the VPP still has the capability to either inject or absorb active power (to respond to market prices) while providing this level of FFR. The VPP's flexibility is also dependent on the VPP's reactive power dispatch point. This highlights the importance of optimizing VPP operation in all markets/services, considering both active and reactive power simultaneously. Making these decisions in a non-holistic manner may reduce the revenue accrued from multi-market participation.

It can be observed by looking at the flexibility maps for Cases 1, 5, and 6 that when resources are aggregated, the resulting FOR is of greater size than the sum of the FORs of each individual resource. This aggregating of resources also dramatically increases the VPP flexibility in the H_2-*P* space. This gives a VPP the ability to vary its hydrogen output whilst maintaining its active power dispatch point. In general, a VPP would want to maximize its hydrogen output for a set active power dispatch, as hydrogen can be monetized. However, if there exist binding constraints on the hydrogen infrastructure (storage size, export limits, etc.), the VPP could utilize its internal flexibility (by modulating internal dispatch factors) to accommodate these constraints while minimizing the effect that this would have on the VPP's electrical operation.

IV. Results

A. Benefits from Multi-market Operation

The VPP revenue changes for the 28 cases with hydrogen price of 2 $/kg or 3 $/kg and FFR contract set at 50% or 33% of PV generation for 2017, as shown in Fig. 3. Except for contractual FFR, the addition of extra markets/services to the VPP portfolio always increases the revenue that the VPP can generate. In fact, without participating in multiple markets, none of the VPP configurations generate sufficient revenue to match their respective EAC, identifying multi-market portfolios as crucial to VPP economic viability.

The largest impact of multi-market participation can be seen when the VPPs add participation in the six contingency FCAS markets to their portfolio. The effect of this can be seen most prominently in VPPs containing a BESS (a resource which derives most of its value from FCAS). Considering a hydrogen price of 3 $/kg in Case 2A, the electrolyser capacity factor is 20.3%. This is close to the capacity factor that would be expected by considering only the wholesale energy prices over the year. In 2017, only 13.4% of price intervals are below the price threshold necessary to sell hydrogen at a profit. The reason in Case 2A where the electrolyser capacity factor is higher than this is due to the contractual arrangement the electrolyser has with the wind farm on node 18 to buy the energy that would otherwise be curtailed. This contract leads to an additional 1.05 M$ of hydrogen revenue in 2017 with a hydrogen price of 3 $/kg. Participation in FCAS also leads to an increase in electrolyser capacity factor of 25.1% in 2017, more than doubling the amount of hydrogen generated and sold in 2017.

In summary, multi-market participation is key to boosting VPP economic viability and can lead to additional hydrogen generation.

B. Sensitivity to Magnitude of Contractual FFR

The only service that can cause a reduction in VPP revenue in these case studies is FFR. This is because this is a contractual arrangement rather than a market where a VPP

can respond to price signals when deciding whether to participate. The VPP configuration that is worst affected by this is Case 2 (only an electrolyser). This is because an electrolyser providing FFR must act as a load at the required magnitude (so that it can be turned off if required to provide the net increase in power output). During these periods of FFR provision, the electrolyser is very limited in how it can respond to the wholesale energy market prices (as explained in Fig. 2 and Section III-C), thus exposing itself to possible high wholesale energy prices. In 2017, providing 50% FFR in Cases 2-5 costs the VPP more than the 1.506 M$ contract price (indicating that the contract has been valued too low for 50%).

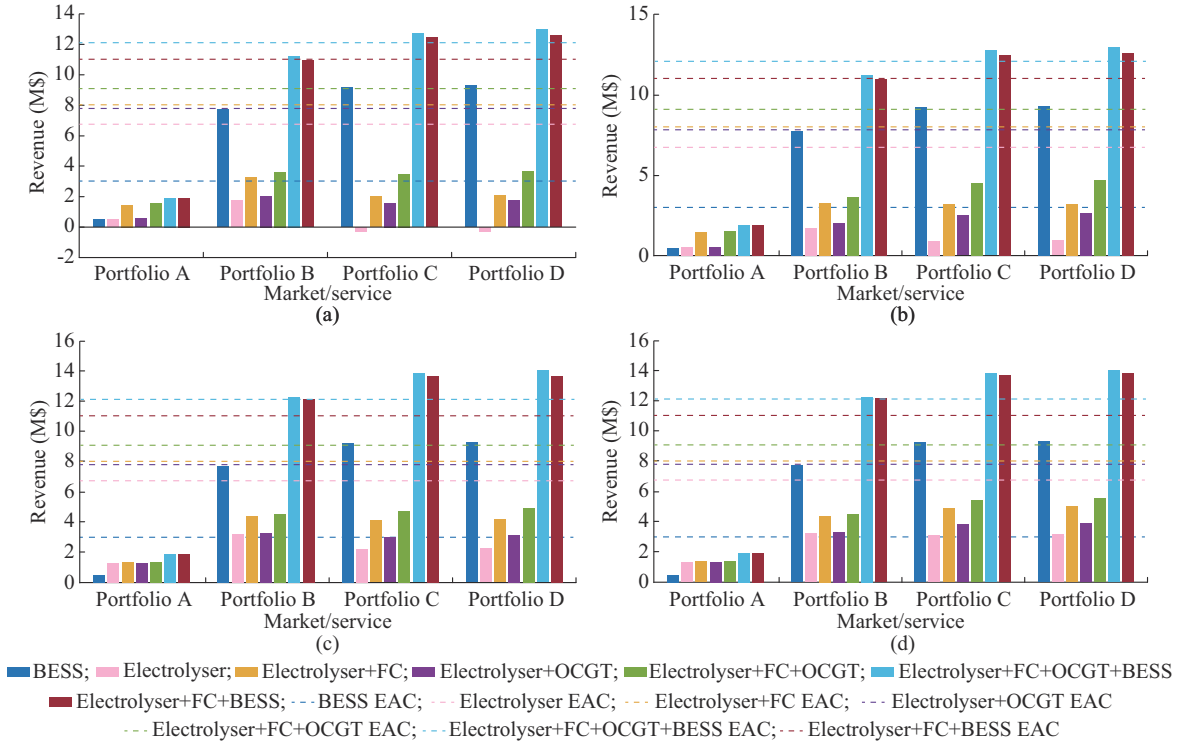

Fig. 3. VPP revenues in 2017 for 50% or 33% contractual FFR provision and hydrogen prices of 2 $/kg or 3 $/kg. (a) 50% FFR and hydrogen price of 2 $/kg. (b) 33% FFR and hydrogen price of 2 $/kg. (c) 50% FFR and hydrogen price of 3 $/kg. (d) 33% FFR and hydrogen price of 3 $/kg.

In summary, VPP operators should carefully consider contractual arrangements they enter into to ensure that they will be profitable, as contracts can require reserving flexibility which could otherwise be used to generate revenue.

C. Sensitivity to Hydrogen Prices

Examining the revenues for different VPP configurations when the hydrogen price is 2 $/kg, as shown in Fig. 3, it is observed that the revenues of Cases 2-5 are below their respective EAC. A reason Cases 6C, 6D, 7C, 7D have revenues greater than the required EAC is because the high FCAS prices allow the BESS to generate very high revenues, compensating for the poor performance of the hydrogen-based devices. The average wholesale energy prices in 2017 is 105.33 $/MWh. These energy prices are too high most of the time for the electrolyser to be able to profitably generate hydrogen. Additionally, the current initial investment cost of a PEM electrolyser is too high for a 2 $/kg hydrogen price to be viable. For the electrolyser and storage system proposed here, if the electrolyser operates with an 85% capacity factor each year, 1.58 $/kg of hydrogen produced would be needed to match the EAC. This only leaves 0.42 $/kg of hydrogen to cover energy procurement costs, which is far below the equivalent wholesale energy prices.

When the hydrogen price is changed to 3 $/kg, there is a large change of hydrogen-based VPP revenues. Increasing the hydrogen price allocates more values to the hydrogen produced when the VPPs are providing FFR services. This is because, for an electrolyser to provide FFR, necessarily it must be on and consuming electricity (as explained in Section III-C), and therefore creating hydrogen. As the price of the fixed-price SPA increases, the value of the hydrogen that is being created as a biproduct of being available to provide FFR also increases.

To summarize, for a hydrogen SPA priced at 3 $/kg and FFR requirement of 33%, all the VPP configurations manage to generate profit from providing FFR when compensated at 1.506 M$/year.

D. Sensitivity to Energy and FCAS Prices

VPP revenue is highly dependent on wholesale energy and FCAS market prices. To further consider the effects of changing wholesale energy and FCAS prices, as well as trends within these markets, case studies are run utilizing the market prices during 2013-2020. Informed by the findings in Fig. 3, these further studies will only consider a hydrogen SPA priced at 3 $/kg and the FFR requirement for the VPP at 33% (where the contract value of $150600 is deemed suit-

able). These studies will look at all seven VPP configurations but will only consider each configuration participating in all markets and services (i. e., Cases 1D-7D), as it has been established that multi-market participation is crucial to maximizing VPP revenue.

Figure 4 shows that BESS revenue is almost entirely from FCAS markets, whereas the hydrogen-based VPPs have a more variable revenue mix. Cases 2-7 in 2013 all generate revenue less than the EAC due to the combination of high energy prices and low FCAS prices. In general, a high average wholesale energy price causes Cases 2-5 to accrue less revenue. Even though 2019 has a high average wholesale energy price, the high FCAS prices allows the VPPs to still make a profit. For comparison, Fig. 4 also provides a "base case" VPP value, which is the value that an electrolyser could accrue each year participating only in the wholesale energy market and fixed price hydrogen contract. This illustrates the additional value available from multi-market participation and aggregation.

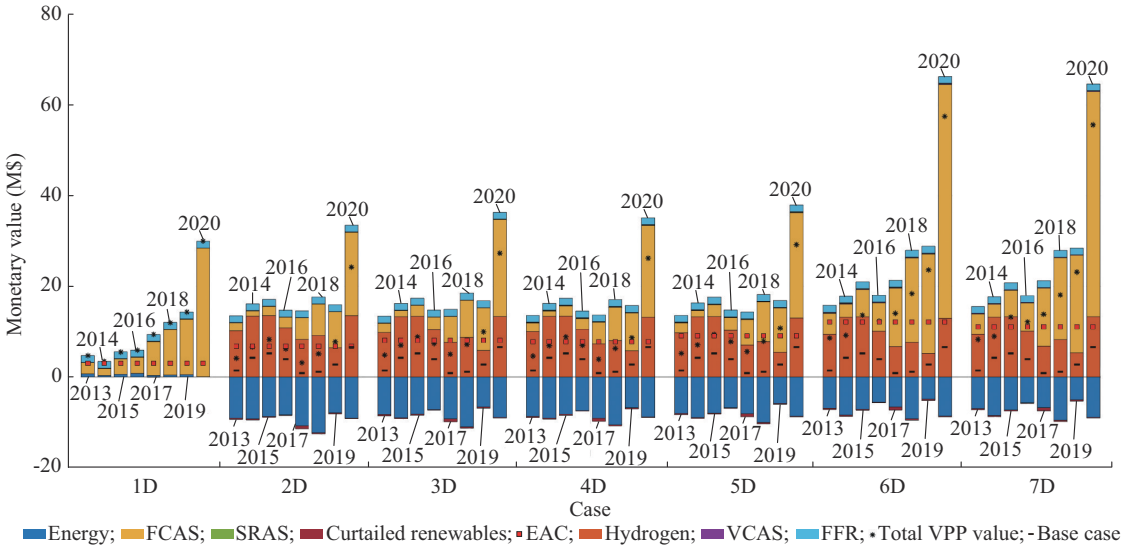

Fig. 4. VPP revenues for 2013-2020 in Cases 1D-7D with hydrogen price of 3 $/kg and FFR requirement of 33% of PV generation.

The significantly higher FCAS prices in 2020 lead to much higher revenue in all configurations. If wholesale energy prices fall in the coming years due to increased RES integration, and FCAS prices continue to rise, then the profits of hydrogen-based VPPs will continue to increase. VCAS and SRAS with the assumed pricing are not significant compared with the other revenues. VCAS revenue varies from $58000-$157000 per year. SRAS when it is provided is worth $103000 per year.

In summary, VPP revenue is highly dependent on market prices, but diversifying market participation helps protect revenue generation from unfavorable conditions in a single market.

To assess the amount of hydrogen that is sold each year, it is compared with the maximum possible sale (i. e., if the electrolyser is operated at the maximum power constantly over the whole year) which we will refer to as the VPP's capacity factor. Table III shows the capacity factors of each electrolyser-based VPP configuration (with a full market/service portfolio) for 2013-2020 and a "business as usual" case. The "business as usual" case considers only an electrolyser and the energy pricing throughout the year. It is assumed that the electrolyser operates at full capacity when the energy price is below the threshold where it can sell hydrogen for a profit at 3 $/kg.

Table III shows that using the VPP to participate in markets/services not only opens additional revenue streams for the VPP, but also allows it to generate and sell more hydrogen. By comparing "business as usual" and Case 2D (in both cases the VPP only contains an electrolyser), the additional hydrogen generated while providing services in Case 2D is worth almost 3 M$/year. Even when the hydrogen is being consumed via the fuel cell and hydrogen OCGT, the average capacity factor of the VPP is still significantly higher than "business as usual".

TABLE III
CAPACITY FACTOR OF EACH ELECTROLYSER-BASED VPP CONFIGURATION FOR 2013-2020 AND A "BUSINESS AS USUAL" CASE

Year	Capacity factor (%)						
	Business as usual	Case 2D	Case 3D	Case 4D	Case 5D	Case 6D	Case 7D
2013	57.8	67.9	65.2	66.9	64.8	62.9	63.0
2014	82.9	89.3	88.4	89.0	88.2	87.6	87.7
2015	86.7	90.0	89.0	89.2	88.7	88.3	88.4
2016	56.6	71.8	69.2	69.9	68.3	67.0	67.1
2017	13.4	55.2	51.2	48.6	46.8	44.9	45.4
2018	15.2	61.0	57.9	53.4	52.1	51.2	54.5
2019	22.2	42.9	38.8	38.5	36.2	34.6	35.3
2020	76.2	89.7	88.5	87.2	86.2	86.0	88.1
Average	51.4	71.0	68.5	67.8	66.4	65.3	66.2

These results highlight that multi-market participation allows additional profitable hydrogen generation, as well as unlocking additional revenue streams.

E. Benefits to Wider Network

The integration of a VPP can have wider network benefits, especially if the network is operating close to design limits (i.e., a congested network due to high RES export). These benefits can only be assessed by using an optimization that models the electrical network, such as the one proposed in this work.

1) Curtailed Renewables

A benefit of the VPP in a congested area of the network is the ability of the VPP to utilize renewable energy that would previously have been curtailed. As an example, in the 2017 "business as usual" case, 17% of the 156820 MWh of energy generated by the wind farm at node 18 would be curtailed due to line thermal limits. In Case 6D in 2017, this amount is reduced to only 4.1% of the wind farm energy curtailed, with the remainder being bought by the VPP to create hydrogen or charge a BESS. This could create over 525000 kg of additional hydrogen in 2017. Using an operational model that captures the local electrical network allows this interaction to be considered.

2) Easing of Network Congestion

One additional benefit of having an electrolyser provide FFR is that it may act to relieve congestion in the wider network, allowing generators to export more energy and accrue higher revenue. In the case studies, this is predominately the OCGTs at nodes 13 and 15. The easing of congestion that the VPPs deliver when providing FFR is worth on average 2.3 M$/year from 2013 to 2020. In this work, there is no mechanism for the VPP to access any of this additional value. However, the agreements could be made to have part of these funds be used to supplement the FFR payment that the VPP receives from the PV generators, leading to additional profits.

F. Value Metrics

The annual revenues obtained from the detailed modelling conducted in this work can be used as an input for cost-benefit analysis to determine if the 3 $/kg fixed-priced contract to sell hydrogen is economically feasible. To assess the economic viability of the proposed VPP configurations and 3 $/kg hydrogen SPA, two value metrics are used, i.e., net present value (NPV) and discounted payback period (DPP).

1) NPV

NPV represents the difference between the expected revenues of a project (converted into "today's money" by using a discount rate) and the amount in initial investment required. In this way, NPV captures the total value of the project. The NPV of each option is calculated using (49).

$$NPV = -CAPEX + \sum_{t=1}^{n} \frac{I_{\text{yearly}} - OPEX}{(1+d)^t} \tag{49}$$

where d is the discount rate of 7%; and n is the number of years considered; and I_{yearly} is the yearly income. The VPP includes devices with 20-40 years' lifetimes. So, a conservative estimate for VPP lifetime of 20 years is considered for this analysis.

2) DPP

Another indicator that can be used to consider the economic viability of investment in a project is the DPP of the investment, which can be determined by (50). The DPP determines how long it takes to recoup the initial investment cost of a project while also incorporating a discount rate to recognize the changing value of money over time.

$$DPP = \frac{1}{\ln(1+d)} \ln\left(\frac{1}{1 - \dfrac{CAPEX \cdot d}{I_{\text{yearly}}}}\right) \tag{50}$$

The NPV and DPP for each VPP configuration with Portfolio D are shown in Table IV. It should be noted that the calculations assume that the average yearly revenue during 2013-2020 shown in Fig. 4 is the VPP yearly income over the lifetime of the VPP. Firstly, in all the VPP configurations, the DPP is less than the assumed 20-year lifetime of the VPP. The NPV is also positive in all cases, indicating that any of these VPP configurations would be an economically viable venture with a 3 $/kg fixed-price hydrogen SPA. Secondly, whilst inclusion of the hydrogen OCGT acts to increase the average yearly revenue, it reduces the NPV of the VPP, and increases the DPP. This indicates that the extra value that the hydrogen OCGT is providing the VPP is not significant enough to offset the required investment. Inclusion of the fuel cell increases the NPV of the VPP (comparing Case 2D and Case 3D); however, it also increases the DPP, although not significantly. The results in Table IV indicate that the solution with the shortest DPP is to install a BESS only. However, the VPP configuration with the highest NPV includes an electrolyser, a fuel cell, hydrogen storage, and a BESS (Case 7D). The DPP for this configuration is longer than for the BESS alone, but it is still well below the VPP lifetime.

TABLE IV
AVERAGE YEARLY REVENUE (2013-2020) OF EACH VPP CONFIGURATION WITH PORTFOLIO, AND THEIR ASSOCIATED NPV AND DPP

Case	Average yearly revenue ($)	NPV ($)	DPP (year)
1D	10630463	80707072	3.20
2D	8167473	12721257	13.55
3D	9669348	15014878	13.60
4D	9039243	8121955	15.98
5D	10368671	8588670	16.26
6D	19657388	75081266	8.40
7D	19143685	83473934	7.34

V. CONCLUSION

The ability to generate hydrogen via electrolysis and predominantly from renewable electricity for 2-3 $/kg is essential for the development of the Australian hydrogen export industry. While previous analysis has determined this is not feasible presently, the more detailed modelling conducted in this work highlights how multi-market/service participation and aggregation into a VPP can allow the sale of hydrogen for 3 $/kg to be economically viable. Furthermore, participating in multiple markets acts to increase the maximum value of wholesale energy below which the VPP can profitably cre-

ate hydrogen. This in turn allows the VPP to create more hydrogen at a lower cost.

However, even with this innovative value-stacking approach, the prices of wholesale energy in the Australian market and the initial investment costs of resources are too high to allow hydrogen to be sold at 2 $/kg. It is important to analyze potential operation over a number of years to determine an accurate value for yearly revenue, as market prices vary greatly between years. The largest hurdle to a VPP's ability to sell hydrogen at 2 $/kg is the current investment cost of the technology. However, as these technologies mature, investment costs will reduce and future multi-energy VPPs will be well placed to generate this low-cost hydrogen, especially if there is a reduction in wholesale energy prices or increase in FCAS prices.

It is worth noting that the competitiveness of hydrogen generated from RES may be increased by external factors, such as the high and volatile gas prices experienced worldwide in 2022. The highly flexible nature of hydrogen-based VPPs will allow them to improve their business cases in more volatile markets. This will act to make hydrogen generated from RES more price-competitive. Additionally, it will mean that using hydrogen to power OCGTs will also become more valuable, as using natural gas becomes more expensive.

REFERENCES

[1] S. Clegg, L. Zhang, and P. Mancarella, "The role of power-to-transport via hydrogen and natural gas vehicles in decarbonising the power and transportation sector," in *Proceedings of IEEE PES Innovative Smart Grid Technologies Conference Europe*, Torino, Italy, Sept. 2017, pp. 1-6.

[2] S. Clegg and P. Mancarella, "Integrated modeling and assessment of the operational impact of power-to-gas (P2G) on electrical and gas transmission networks," *IEEE Transactions on Sustainable Energy*, vol. 6, no. 4, pp. 1234-1244, May 2015.

[3] M. Yu, K. Wang, and H. Vredenburg, "Insights into low-carbon hydrogen production methods: green, blue and aqua hydrogen," *International Journal of Hydrogen Energy*, vol. 46, no. 41, pp. 21261-21273, Jun. 2021.

[4] S. Bruce. (2018, Dec.). National hydrogen roadmap, CSIRO, Newcastle, Australia. [Online]. Available: https://www. csiro. au/-/media/Do-Business/Files/Futures/180314_EN_NationalHydrogen Roadmap_W EB_180823.pdf

[5] X. Li and M. Mulder, "Value of power-to-gas as a flexibility option in integrated electricity and hydrogen markets," *Applied Energy*, vol. 304, p. 117863, Dec. 2021.

[6] G. Chicco, S. Riaz, A. Mazza *et al*., "Flexibility from distributed multienergy systems," *Proceedings of the IEEE*, vol. 108, no. 9, pp. 1496-1517, Apr. 2020.

[7] E. Corsetti, S. Riaz, M. Riello *et al.*, "Modelling and deploying multi-energy flexibility: the energy lattice framework," *Advances in Applied Energy*, vol. 2, p. 100030, May 2021.

[8] H. Khani, N. A. El-Taweel, and H. E. Z. Farag, "Supervisory scheduling of storage-based hydrogen fueling stations for transportation sector and distributed operating reserve in electricity markets," *IEEE Transactions on Industrial Informatics*, vol. 16, no. 3, pp. 1529-1538, Mar. 2020.

[9] N. A. El-Taweel, H. Khani, and H. E. Z. Farag, "Hydrogen storage optimal scheduling for fuel supply and capacity-based demand response program under dynamic hydrogen pricing," *IEEE Transactions on Smart Grid*, vol. 10, no. 4, pp. 4531-4542, Jul. 2019.

[10] L. Zhang, S. Clegg, and P. Mancarella, "Modeling of electrolyzers in hydrogen vehicle refueling stations for provision of ancillary services," in *Proceedings of Bulk Power Systems Dynamics and Control Symposium*, Espinho, Portugal, Sept. 2015, pp. 1-6.

[11] B. A. Robbins and A. D. Domínguez-García, "Optimal reactive power dispatch for voltage regulation in unbalanced distribution systems," *IEEE Transactions on Power Systems*, vol. 31, no. 4, pp. 2903-2913, Jul. 2016.

[12] B. Zhang, A. Y. S. Lam, A. D. Domínguez-García *et al.*, "An optimal and distributed method for voltage regulation in power distribution systems," *IEEE Transactions on Power Systems*, vol. 30, no. 4, pp. 1714-1726, Jul. 2015.

[13] E. Dall'Anese, S. V. Dhople, and G. B. Giannakis, "Optimal dispatch of photovoltaic inverters in residential distribution systems," *IEEE Transactions on Sustainable Energy*, vol. 5, no. 2, pp. 487-497, Jan. 2014.

[14] N. Ruiz, I. Cobelo, and J. Oyarzabal, "A direct load control model for virtual power plant management," *IEEE Transactions on Power Systems*, vol. 24, no. 2, pp. 959-966, May 2009.

[15] C. Suazo-Martinez, E. Pereira-Bonvallet, R. Palma-Behnke *et al.*, "Impacts of energy storage on short term operation planning under centralized spot markets," *IEEE Transactions on Smart Grid*, vol. 5, no. 2, pp. 1110-1118, Mar. 2014.

[16] M. Tostado-Véliz, P. Arévalo, and F. Jurado, "A comprehensive electrical-gas-hydrogen microgrid model for energy management applications," *Energy Conversion and Management*, vol. 228, p. 113726, Jan. 2021.

[17] M. A. Pellow, C. J. M. Emmott, C. J. Barnhart *et al.*, "Hydrogen or batteries for grid storage? A net energy analysis," *Energy & Environmental Science*, vol. 8, no. 7, pp. 1938-1952, Apr. 2015.

[18] H. Fu, Z. Wu, X.-P. Zhang *et al.*, "Contributing to DSO's energy-reserve pool: a chance-constrained two-stage VPP bidding strategy," *IEEE Power and Energy Technology Systems Journal*, vol. 4, no. 4, pp. 94-105, Dec. 2017.

[19] J. Naughton, H. Wang, S. Riaz *et al.*, "Optimization of multi-energy virtual power plants for providing multiple market and local network services," *Electric Power Systems Research*, vol. 189, p. 106775, Dec. 2020.

[20] E. A. M. Ceseña, N. Good, A. L. A. Syrri *et al.*, "Techno-economic and business case assessment of multi-energy microgrids with co-optimization of energy, reserve and reliability services," *Applied Energy*, vol. 210, pp. 896-913, Jan. 2018.

[21] R. Moreno, R. Moreira, and G. Strbac, "A MILP model for optimising multi-service portfolios of distributed energy storage," *Applied Energy*, vol. 137, pp. 554-566, Jan. 2015.

[22] D. Kroniger and R. Madlener, "Hydrogen storage for wind parks: a real options evaluation for an optimal investment in more flexibility," *Applied Energy*, vol. 136, pp. 931-946, Dec. 2014.

[23] S. McDonagh, S. Ahmed, C. Desmond *et al.*, "Hydrogen from offshore wind: Investor perspective on the profitability of a hybrid system including for curtailment," *Applied Energy*, vol. 265, p. 114732, May 2020.

[24] M. Eypasch, M Schimpe, A. Kanwar *et al.*, "Model-based techno-economic evaluation of an electricity storage system based on liquid organic hydrogen carriers," *Applied Energy*, vol. 185, pp. 320-330, Jan. 2017.

[25] L. Weimann, P. Gabrielli, A. Boldrini *et al.*, "Optimal hydrogen production in a wind-dominated zero-emission energy system," *Advances in Applied Energy*, vol. 3, p. 100032, Aug. 2021.

[26] A. Rabiee, A. Keane, and A. Soroudi, "Technical barriers for harnessing the green hydrogen: a power system perspective," *Renewable Energy*, vol. 163, pp. 1580-1587, Aug. 2021.

[27] W. Sun and G. P. Harrison, "Active load management of hydrogen refuelling stations for increasing the grid integration of renewable generation," *IEEE Access*, vol. 9, pp. 101681-101694, Jul. 2021.

[28] J. Yang, Z. Ning, C. Kang *et al*., "A state-independent linear power flow model with accurate estimation of voltage magnitude," *IEEE Transactions on Power Systems*, vol. 32, no. 5, pp. 3607-3617, Sept. 2017.

[29] J. Naughton, H. Wang, M. Cantoni *et al*., "Co-optimizing virtual power plant services under uncertainty: a robust scheduling and receding horizon dispatch approach," *IEEE Transactions on Power Systems*, vol. 36, no. 5, pp. 3960-3972, Sept. 2021.

[30] S. Riaz, G. Verbič, and A. C. Chapman, "Computationally efficient market simulation tool for future grid scenario analysis," *IEEE Transactions on Smart Grid*, vol. 10, no. 2, pp. 1405-1416, Mar. 2019.

[31] A. de Corato, I. Saedi, S. Riaz *et al*., "Aggregated flexibility from multiple power-to-gas units in integrated electricity-gas-hydrogen distribution systems," *Electric Power Systems Research*, vol. 212, p. 108409, Nov. 2022.

[32] T. S. Brinsmead, P. Graham, J. Hayward *et al*. (2015, Sept.). Future energy trends: an assessment of the economic viability, potential uptake and impacts of electrical energy storage on the NEM 2015-2035.

CSIRO. Newcastle, Australia. [Online]. Available: https://www.aemc.gov.au/sites/default/files/content/fa7a8ca4-5912-4fa9-8d51-2f291f7b9621/CSIRO-Future-Trends-Report.pdf
[33] McKinsay & Company. (2021, Feb.). Hydrogen insights: a perspective on hydrogen investment, market development and cost competitiveness. [Online]. Available: https://hydrogencouncil. com/wp-content/uploads/2021/02/Hydrogen-Insights-2021.pdf
[34] S. Moss. (2019, Dec.). 2019 costs and technical parameter review, Aurecon Australasia Pty Ltd. Brisbane, Australia. [Online]. Available: https://www.aemo.com.au/-/media/Files/Electricity/NEM/Planning_and_Forecasting/Inputs-Assumptions-Methodologies/2019/Aurecon-2019-Cost-and-Technical-Parameters-Review-Draft-Report.PDF
[35] Australian Energy Market Operator. (2021, Dec.). Market data: NEMWEB. Australian Energy Market Operator, Melbourne, Australia. [Online]. Available: http://www.nemweb.com.au
[36] Australian Government: Bureau of Meterology. (2021, Dec.). About one minute solar data. [Online]. Available: http://www.bom.gov.au/climate/data/oneminsolar/about-IDCJAC0022.shtml
[37] SA Power Networks. (2021, Dec.). Resource library. [Online]. Available: https://www.sapowernetworks.com.au/resource-library
[38] *Electricity Connection for Retail Customers*, National Electricity Rules 5.3A.12(a), 2022.
[39] Australian Energy Market Commission. (2020, Dec.). Frequency control rule changes, Sydney, Australia. [Online]. Available: https://www.aemc.gov.au/sites/default/files/2020-12/Frequency%2 0control%20rule%20changes%20-%20Directions%20paper%20-%20December%202020.pdf
[40] C. Christiansen and N. Hillmann. (2017, Jun.). Feasibility of fast frequency response obligations of new generators, AECOM Australia Pty Ltd. Sydney, Australia. [Online]. Available: https://www.aemc.gov.au/sites/default/files/content/661d5402-3ce5-4775-bb8a-9965f6d93a94/AECOM-Report-Feasibility-of-FFR-Obligations-of-New-Generators.pdf
[41] M. Gatt. (2022, May). Power system security guidlines. Australian Energy Market Operator. Melbourne, Australia. [Online]. Available: https://www.aemo.com.au/-/media/Files/Electricity/NEM/Security_and_ Reliability/Power_System_Ops/Procedures/SO_OP_3715---Power-System-Security-Guidelines.pdf
[42] Australian Energy Market Operator. (2019, Dec.). 2019 network support and control ancillary services (NSCAS) report, Australian Energy Market Operator, Melbourne, Australia. [Online]. Available: https://aemo. com. au/-/media/files/electricity/nem/planning_and_ forecasting/isp/2019/2019_nscas_report.pdf?la=en
[43] M. Gatt. (2021, Feb.). SRAS guideline: system restart ancillary services incorporating boundaries of electrical sub networks, Australian Energy Market Operator, Melbourne, Australia. [Online]. Available: https://aemo. com. au/-/media/files/electricity/nem/security_and_ reliability/ancillary_services/sras/sras-guideline-2021.pdf?la=en
[44] Australian Energy Market Operator. (2021, Feb.). Non-market ancillary services (NMAS) cost and quantity report 2019-2020, Australian Energy Market Operator. Melbourne, Australia. [Online]. Available: https://aemo. com. au/-/media/files/electricity/nem/data/ancillary_services/2021/nmas-cost-and-quantities-report-2019-20.pdf?la=en

James Naughton received the M.Eng. degree from the University of Southampton, Southampton, UK, in 2015, and the Ph.D. degree jointly from the University of Melbourne, Melbourne, Australia and the University of Birmingham, Birmingham, UK, in 2022. He is currently a Research Fellow at the Department of Electrical and Electronic Engineering, The University of Melbourne. His research interests include modelling and optimization of distributed energy resource (DER) operation in multi-energy systems, and design of DER marketplaces.

Shariq Riaz received the B.Sc. (Hons.) and M.Sc. degrees in electrical engineering from the University of Engineering and Technology Lahore, Lahore, Pakistan, in 2009 and 2012, respectively, and the Ph. D. degree from The University of Sydney, Sydney, Australia, in 2018. He is currently a Research Fellow with the Power and Energy Systems Group, The University of Melbourne, Melbourne, Australia. He has expertise in power system operation and electricity markets. His current research interests include flexibility from distributed energy resources, multi-energy systems, and distributed energy marketplaces.

Michael Cantoni received the B. E. (Hons.) and B. Sc. degrees from The University of Western Australia, Perth, Australia, in 1995, and the Ph.D. degree from The University of Cambridge, Cambridge, UK, in 1998. He joined The University of Melbourne, Melbourne, Australia, in 2000, where is currently a Full Professor in the Department of Electrical and Electronic Engineering. He held post-doctoral research positions at The University of Cambridge, Cambridge, UK, in 1998-2000, and a visiting academic position at Imperial College London, London, UK, in 2019-2020. He received the IEEE Control Systems Technology Award in 2014 for the development and implementation of controls for irrigation channels and water management with an industry partner. He has served as Associate Editor for IFAC Automatica, Systems & Control Letters, IET Control Theory and Applications, and the Springer Reference Works Encyclopedia of Systems and Control. His research interests include robust and optimal control, sampled-data and networked systems, and applications in water and power networks.

Xiao-Ping Zhang received the B.Eng., M.Sc., and Ph.D. degrees in electrical engineering from Southeast University, Nanjing, China, in 1988, 1990, and 1993, respectively. He was an Associate Professor with the University of Warwick, Coventry, UK. From 1993 to 1998, he was with the NARI Group Corporation (State Grid Electric Power Research Institute) on EMS/DMS advanced application software research and development. From 1998 to 1999, he was visiting University of Manchester Institute of Science and Technology (UMIST), Manchester, UK. From 1999 to 2000, he was an Alexander-von-Humboldt Research Fellow with the University of Dortmund, Dortmund, Germany. He is currently a Professor of electrical power systems with the University of Birmingham, Birmingham, UK. He is also the Director of the Smart Grid, Birmingham Energy Institute. He has coauthored the first and second edition of the monograph Flexible AC Transmission Systems: Modelling and Control (Springer, in 2006 and 2012). He has coauthored the book Restructured Electric Power Systems: Analysis of Electricity Markets with Equilibrium Models (IEEE Press/Wiley, in 2010). He has been made a Fellow of IEEE for contributions to modeling and control of high-voltage DC and AC transmission systems. He is an IEEE PES Distinguished Lecturer on high-voltage direct current (HVDC), flexible alternating current transmission system (FACTS), and wave energy generation. He is the Chair of the IEEE WG on Test Systems for Economic Analysis. He is an Advisor to the IEEE PES UK and Ireland Chapter. His research interests include modeling and control of HVDC, FACTS and renewable energy, distributed generation control, energy market operations, and power system planning.

Pierluigi Mancarella received the M.Sc. and Ph.D. degrees in electrical energy systems from the Politecnico di Torino, Turin, Italy, in 2002 and 2006, respectively. He is currently the Chair Professor of electrical power systems at The University of Melbourne, Melbourne, Australia, and Professor of smart energy systems at The University of Manchester, Manchester, UK. He is an Editor of the IEEE Transactions on Power Systems and of the IEEE Transactions on Energy Markets, Policy and Regulation, an IEEE Power and Energy Society Distinguished Lecturer, and the Convenor of the CIGRE Working Group C6/C2.34 “Flexibility provision from distributed energy resources”. His research interests include multi-energy systems, grid integration of renewables, energy infrastructure planning under uncertainty, and resilience of low-carbon networks.